FTUV/97-40
IFIC/97-40
UG-DFM-5/97

Inclusive $(e, e'N)$, $(e, e'NN)$, $(e, e'\pi)$ ... reactions in nuclei

A. Gil[1], J. Nieves[2] and E. Oset[1]

[1] *Departamento de Física Teórica and IFIC, Centro Mixto Universidad de Valencia - CSIC, 46100 Burjassot (Valencia) Spain.*

[2] *Departamento de Física Moderna, Universidad de Granada, 18071 Granada, Spain.*

Abstract

We study the inclusive $(e, e'N)$, $(e, e'NN)$, $(e, e'\pi)$, $(e, e'\pi N)$ reactions in nuclei using a Monte Carlo simulation method to treat the multichannel problem of the final state. The input consists of reaction probabilities for the different steps evaluated using microscopical many body methods.

We obtain a good agreement with experiment in some channels where there is data and make predictions for other channels which are presently under investigation in several electron laboratories. The comparison of the theoretical results with experiment for several kinematical conditions and diverse channels can serve to learn about different physical processes ocurring in the reaction. The potential of this theoretical tool to make prospections for possible experiments, aiming at pinning down certain reaction probabilities, is also emphasized.

PACS: 21.60.Ka, 24.10.Cn, 25.30.Fj, 25.30.Rw

1 Introduction

Experiments on exclusive (e, e') reactions in nuclei are becoming more and more common in present electron laboratories. Experiments concentrate on $(e, e'p)$, $(e, e'NN)$, $(e, e'\pi)$, $(e, e'\pi N)$ etc. reactions which, together with the inclusive (e, e') measurements should help us understand better the mechanisms of nuclear excitation by electromagnetic probes. Proton knockout reactions at low energies have been used as tools to learn about nuclear structure, high momentum components in the nucleus, nuclear correlations, etc. [1, 2, 3, 4, 5]. Two nucleon emission reactions have been encouraged with the hope that they can teach us something about nuclear correlations [3, 6, 7].

However, meson exchange currents mechanisms and delta excitation are usually competitive and, together with complications in dealing with final state interactions, make the extraction of information on nuclear correlations a difficult task [3].

Mechanisms for 2N emission in (e, e') reactions have been developed in [8, 9] and [10, 11]. The analogous reaction of two nucleon emission induced by real photons has received parallel attention [12, 13, 14]. The approaches of the Pavia [8, 9, 13] and Gent groups [10, 11] are suited to deal with low energy photons, below the pion emission threshold which opens new channels for 2N emission [14]. Both groups take into account final state interactions of the two nucleons with the nucleus: the Pavia group by means of nucleon distorted waves with a complex optical potential, while the Gent group uses a real nucleon-nucleus potential. The distortion of the nucleon wave function by a complex optical potential removes all events where the nucleons collide with other nucleons. The procedure is suited to study NN emission leading to specific final nuclear states. However, if one is interested in "inclusive" 2N emission, meaning that one wishes to compare with an experiment where 2N are detected but one is implicitly summing over all final nuclear states, including more than 2N emission, one has to find a different scheme. The distortion by a real potential does not eliminate the events where there are nucleon collisions. On the other hand, it does not account either for events coming from one nucleon emission followed by secondary collisions of the nucleon which lead to two or more nucleon emission. Such events have been taken into account in ref. [15] although they are insufficient to account for the 2N spectra. This sort of final state interaction is also adressed in [16] in order to account for contributions to $(e, e'pp)$ from $(e, e'pn)$ followed by charge exchange in a secondary collision of the neutron. However, only analogue intermediate states are allowed to be excited in that approach and in nuclei with $T = 0$ there is no contribution from this channel. None of the above mentioned approaches deals explicitly with pion production and hence they miss the most important channel of 2N emission at energies above $E_\gamma = 250\, MeV$ which consists of real pion creation followed by the absorption of the pion on its way out the nucleus (indirect photon absorption) [14]. In ref. [14] a thorough work was done for γ absorption in nuclei, including all possible many step processes: a) photon absorption by a pair of nucleons, b) photon absorption by a trio of nucleons, c) (γ, π) at a point in the nucleus followed by pion and nucleon collisions, d) (γ, π) followed by pion absorption on its way out of the nucleus, etc. The work uses probabilities of photon absorption or pion photoproduction as input, calculated with a microscopic many body approach [17]. Then in a second step, it uses a Monte Carlo simulation approach to account for the possible reactions which can take place in the interaction of the particles produced with the nucleus. The approach is rather succesful in reproducing the (γ, pn) cross sections [18, 19, 20] although it has some difficulties in the (γ, pp) channel which experimentally shows a very small cross section. Similarly the agreement with the (γ, π) [21] and $(\gamma, \pi N)$ [18] channels is also quite good [22].

The work of ref. [17] has been recently extended to virtual photons in order to study the (e, e') inclusive reaction [23]. On top of several subtleties of virtual photons, the extension of the microscopic many body work of [17] requires the study of the quasielastic channel, $\gamma^* N \to N$, which is absent in real photons (at photon energies bigger than 100 MeV, in practical terms). The work of [23] evaluates the inclusive

(e,e') cross section and at the same time all the probabilities for the reactions that take place in the interaction of γ^* with the nucleons in the first step: (γ^*,π), (γ^*,N), (γ^*,NN) and (γ^*,NNN).

The agreement of the results of ref. [23] with the inclusive (e,e') data is quite good, but since the theory is able to relate the strength of the cross section to different physical channels, the theory has a higher potential predictive power than just the prediction of the strength of the total cross section and it is the purpose of the present paper to exploit this potential.

In the next section we summarize the technical details which are used in [23] in order to obtain the probabilities.

The present work hence aims to get a complete description of all processes which can occur in the (e,e') reaction in nuclei in a range of energies between 100 MeV and about 600 MeV of the virtual photon. These are typical energies of the Mainz facility. In this way we shall evaluate cross sections for $(e,e'N)$, $(e,e'NN)$, $(e,e'\pi)$, $(e,e'\pi N)$ etc. reactions and will compare them with some experiments in order to interprete the data and relate them to the relevant physical mechanisms of the reaction.

2 The evaluation of probabilities in the first step

In a previous paper [23] we carried out a thorough evaluation of the different mechanisms entering the (e,e') inclusive reaction. This allowed us to compare with the inclusive cross section $d^2\sigma/d\Omega' dE'$ (Ω', E' solid angle and energy of the outgoing electron) and also with the longitudinal and transverse response functions. The agreement with the data in the regions of the quasielastic peak, the dip region and the Δ peak is good. On the other hand there is also agreement with the longitudinal and transverse response functions, particularly with the latest analysis of [24] taking the world data.

The study of [23] was done in a covariant way and the response functions are associated to the virtual photon self-energy. Thus,

$$\begin{aligned} W_L &= \frac{q^2}{\pi e^2 |\vec{q}|^2} \int d^3r Im\Pi^{00}(q,\rho(\vec{r})) \\ W_T &= -\frac{1}{\pi e^2} \int d^3r Im\Pi^{xx}(q,\rho(\vec{r})) \end{aligned} \tag{1}$$

Furthermore, the many body techniques used there, as it was the case before in the study of the different reaction channels in pion-nucleus [25] and real photon-nucleus reaction [17], allow one to separate the different contributions to $Im\Pi^{\mu\nu}$ and associate them to the different reaction channels in the first step of the reaction. In order to make the statement more explicit, let us briefly discuss the origin and the separation of these contributions. In ref. [23] we introduced in a systematic way processes which involve $1p1h$ excitation, $2p2h$ excitation, $3p3h$ excitation, $1p1h1\pi$ excitation and $2p2h1\pi$ excitation. Some of the Feynman diagrams which give rise to $Im\Pi^{\mu\nu}$ are drawn in fig. 1.

The imaginary part from a Feynamn diagram is evaluated according to Cutkosky rules. The rules [26] essentially consist of the following: we cut the intermediate states with a line at equal times and when all these states are placed on shell in the integrations over the internal variables, this contributes to $Im\Pi^{\mu\nu}$. Placing on shell a particle means that we take the imaginary part of its propagator. For instance, for a pion

$$D(q) \to 2\,i\,\Theta(q^0) ImD(q) \;=\; 2\,i\,\Theta(q^0)\,(-\pi)\,\delta(q^2 - m_\pi^2) \tag{2}$$

and we see technically the meaning of placing the particle on shell. This way of getting $Im\Pi^{\mu\nu}$ is doubly rewarding. First, because of the economy versus the equivalent and more laborious way (used in fact to prove the Cutkosky rules) of using Wick rotations or other alternative methods. Second, because placing some intermediate particles on shell is telling us which channel of the total cross section we are considering. Cutkosky rules are intimately associated to the optical theorem which relates the total cross section to the imaginary part of the forward elastic scattering amplitude. Here it is the same: one is relating the imaginary part of the self-energy (also forward) to the probability of reaction. Then, the different cuts of intermediate states and their corresponding contribution to $Im\Pi^{\mu\nu}$, provide us with the physical channels of the reaction and the corresponding contribution of these channels to the reaction probability, respectively.

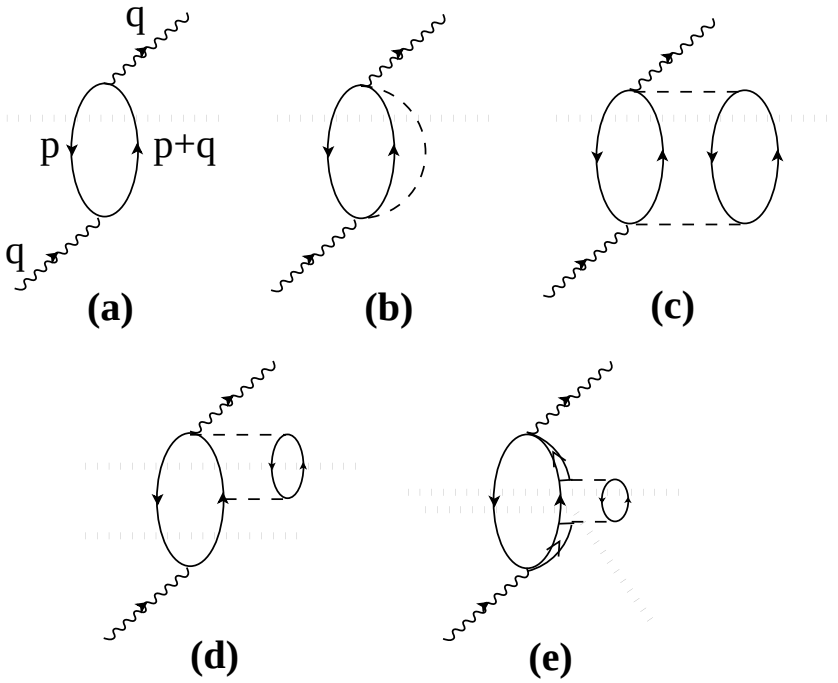

Fig.1 Some many body Feynman diagrams whose imaginary parts contribute to the total inclusive $(e, e'X)$ cross section. The dotted lines indicate which particles are put on shell when evaluating the imaginary part of each diagram.

If we look at fig. 1 we can see the different sources of imaginary part represented by the cuts of the horizontal lines. Hence, in diagram (a) the cut represents the channel of $1p1h$ excitation or absorption of the photon by one nucleon. The reaction probability

associated to this diagram, or equivalently, its contribution to W_L and W_T is calculated in ref. [23]. Here we would like on top of that to have the distribution of momenta of the outgoing nucleon. This can be done by not performing the integration over the momentum of the nucleon occupied states in [23] since p'_N for the outgoing nucleon is $p+q$. However, since we generate events probabilistically one by one, we choose the alternative procedure of generating a random momentum from the local Fermi sea, and this will generate an outgoing momentum $p'_N = p_N + q$ ($p_N \equiv p$ in fig.1). If it happens that $|\vec{p}\,'_N| < k_F(r)$ (the local Fermi momentum) then the event is Pauli blocked, it is dismissed and another event is generated. Thus, we have already the configuration of the final state after the first step: in this case just one nucleon produced in the point $\vec{r}$ of the nucleus with momentum $\vec{p}\,'_N$. As with respect to having a proton and a neutron in the final state, this is trivially done, since the contribution of diagram 1(a) in ref. [23] was already splitted into a proton and a neutron induced ones (see eq. (71) of ref. [23]).

In diagram (b) the cut represents $1p1h1\pi$ excitation or, what is the same, the first step in (γ^*, π). Here we have a probability for this to occur, which is evaluated in [23] and now one has to generate events with a momentum p'_N and p_π for the outgoing N and π. These momenta are generated according to the weight that they have in the evaluation of the probability, which actually involves integrations over these momenta. The technical way to do it is using the random procedure which will be shown later on.

The diagram (c) has a cut corresponding to $2p2h$ excitation. Here the channel represented by this cut is two nucleon emission in the first step. Again we will have to determine the outgoing nucleon momenta through a random procedure but weighed by the momenta distribution implicit in the formulae which evaluate the probabilities by integration over these momenta.

In diagram (d) there is a novelty, peculiar to virtual photons. Indeed, the diagram has actually two sources of imaginary part, one of them corresponding to the upper cut, where we have a $2p2h$ excitation and another one corresponding to the lower cut where we have $1p1h$ excitation. The lower cut has the same structure as (a) and can be cast together using the structure of (a) but with the upper vertex renormalized. In this case we have 1 particle emission. However, the upper cut would contribute to $2N$ emission.

Finally, the diagram (e) contains two cuts, the upper one which corresponds to $2p2h$ excitation, or $2N$ emission, and the lower one, which appears because we have a full (non- static) pion propagator, and which corresponds to having $1p1h1\pi$ excitation, or equivalently, $1N$ and 1π emission.

These diagrams, and the corresponding distributions of pions and nucleons that we get from them, provide the configuration of the final particles after the first step of the collision. Thus we have a set of nucleons and pions with definite momenta produced at the point $\vec{r}$ of the nucleus. These particles still have to cross the nucleus before they are eventually detected, but in their way out the nucleus they can undergo different reactions with other nucleons, thus changing their momenta and leading to the ejection of more nucleons. These secondary steps will be followed by means of a Monte Carlo simulation method and will be discussed in forthcoming sections.

3 The Monte Carlo simulation

3.1 Generating and tracing the pions

Let us assume that one pion is produced in a nuclear element of volume, d^3r. Our simulation procedure allows us to decide (depending on the corresponding probabilities): first, via which process the pion has been produced and its position inside the nucleus. Second, the charge and momentum of the produced pion.

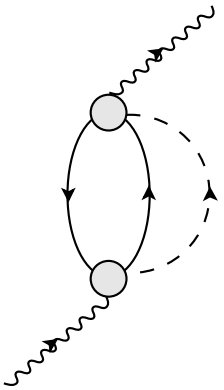

Fig.2 Lowest order contribution to the pion production channel. The dot stands for the full $\gamma^* N \to N\pi$ T-matrix, taken from the model of ref. [23].

As we have shown in a previous paper [23] the pion production channel has different sources: **(a)** the contribution of the diagrams depicted in fig. 2, **(b)** the quasielastic contribution of the Δ piece (fig. 3) and, finally, **(c)** the contribution of the diagram depicted in fig. 4 which is related to the $(\gamma^*, \pi\pi)$ channel. Obviously, as we discussed in [23], the main contribution corresponds to diagrams **(a)**.

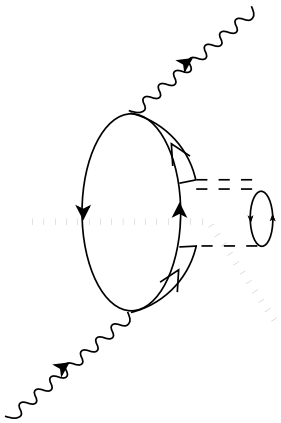

Fig.3 Contribution of the Δ-self-energy in the nuclear medium to the pion production channel.

We evaluate the contribution of the diagrams **(a)** by using the elementary cross section for $\gamma^* N \to N\pi$ and taking into account nuclear medium effects: Fermi motion of the nucleons, modification of the Δ width in the nuclear medium and the corresponding renormalization of the different terms.

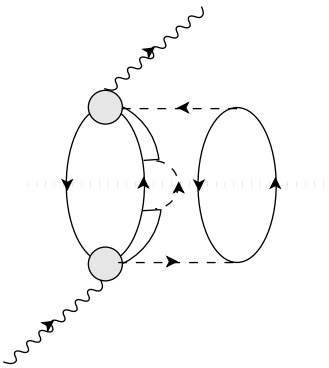

Fig.4 Contribution to the 2p2h1π channel obtained from the $\gamma^* N \to N\pi\pi$ T-matrix (full circle) used in ref. [23].

In ref. [23] we calculate $d\sigma/d\Omega' dE'$, for the (e, e') reaction. We shall refer to it as the γ^* cross section. In particular the contribution of the (γ^*, π) channel from the diagrams **(a)** will be given by:

$$\begin{aligned}\frac{d\sigma_a^\lambda}{d\Omega' dE'} = & \int d^3r \frac{d^3p}{(2\pi)^3} d\Omega^*_{CM} \Theta(cos\,\theta_{Max} - cos\,\theta_{CM}) \frac{|\vec{q}_l|}{|\vec{q}|} \times \\ & \times 2 \left[n_p(\vec{p}) \frac{d\sigma(\gamma^* p)^\lambda}{d\Omega' dE' d\Omega^*_{CM}} + n_n(\vec{p}) \frac{d\sigma(\gamma^* n)^\lambda}{d\Omega' dE' d\Omega^*{}_{CM}} \right]\end{aligned} \tag{3}$$

where $\int d^3r$ is extended to the nuclear volume; $\int d^3p$ corresponds to the integration over the nucleon momenta; n_p and n_n are the proton and neutron occupation numbers; $\Theta(cos\,\theta_{Max} - cos\,\theta_{CM})$ is imposed by Pauli blocking (see ref. [22]) and Ω^*_{CM} is the solid angle of the pion in the CM of the $\gamma^* N$ frame. The index λ stand for the charge of the pion. The factor $|\vec{q}_l|/|\vec{q}|$ is related to the different flux of particles in the nuclear frame and in the nucleon frame ($|\vec{q}_l\,|$ is the photon lab momentum in the $\gamma^* N$ system and $|\vec{q}|$, the momentum in the nuclear system) and it is actually very close to unity [22].

Contributions **(b)** and **(c)** mentioned before need at least two nucleons and they present a ρ^2 dependence in the limit of small densities. We calculate these contributions following the procedure explained in ref. [23]:

$$\frac{d^2\sigma^\lambda_{b,c}}{d\Omega' dE'} = -\frac{\alpha}{q^4} \frac{|\vec{k}'|}{|\vec{k}|} \frac{1}{(2\pi)^2} \int d^3r \left(Im\Pi^{\mu\nu}_{\gamma\,(b,c)} L_{\mu\nu} \right) P_\lambda \tag{4}$$

where P_λ is the probability related to the charge λ of the pion (i.e., the isospin dependence). For **(c)** these probabilities are:

$$P_0(\pi^0) = \frac{2}{12} \;\; ; \;\; P_\pm(\pi^\pm) = \frac{5}{12} \mp \frac{4}{12} \frac{N - Z}{A} \tag{5}$$

And for **(b)** , we consider the probability corresponding to a resonant reaction (γ^*, π) with a renormalized pion (because this is the main contribution):

$$P_0(\pi^0) = \frac{2}{3} \; ; \; P_+(\pi^+) = \frac{Z}{3A} \; ; \; P_-(\pi^-) = \frac{N}{3A} \tag{6}$$

Once the pion is produced, one must decide which process took place ((**a**),(**b**) or (**c**)). If we write:

$$\frac{d^2\sigma^\lambda}{d\Omega' dE'} = \sum_j \frac{d^2\sigma_j^\lambda}{d\Omega' dE'} \tag{7}$$

where the sum over j stands for the **(a)**, **(b)** and **(c)** mechanisms given in eqs. (3),(4). The choice of the process is made according to these $d^2\sigma_j^\lambda/d\Omega' dE'$.

The angular distributions (θ, ϕ) for pions in cases **(a)** and **(b)** are generated according to the differential cross section $d\sigma(\gamma^* N \to \pi N)/d\Omega' dE' d\Omega^*_{CM}$ which appears in eq.(3), while for the case of **(c)** we consider the momenta distributions given by three-body phase space.

As we can see from eqs.(3),(4), the spatial location of each event is easily generated, because the cross section is expressed in terms of probabilities by unit of volume.

Let us show how the selection of $\vec{r}$ and angle is made for the mechanisms **(a)** and **(b)** (in case **(c)** would be done analogously following the phase space distributions). We define for each channel of charge:

$$\begin{aligned}
f(\vec{r}) \quad &/ \quad \frac{d\sigma^\lambda_{(a),(b)}}{d\Omega' dE'} = \int_0^\infty dr\, f(r) \\
g_r(cos\,\theta) \quad &/ \quad f(r) = \int_{-1}^{+1} d(cos\theta)\, g_r(cos\,\theta) \\
t_{r,\theta}(\phi) \quad &/ \quad g_r(cos\,\theta) = \int_0^{2\pi} d\phi\, t_{r,\theta}(\phi) \\
F(r) \quad &= \quad \int_0^r dr'\, f(r') \\
G(cos\,\theta) \quad &= \quad \int_{-1}^{cos\,\theta} d(cos\theta')\, g_r(\cos\theta') \\
T(\phi) \quad &= \quad \int_0^\phi d\phi'\, t_{r,\theta}(\phi')
\end{aligned} \tag{8}$$

We generate three random numbers x,y,$z \in [0, 1[$ and choose one nuclear radius r such that $F(r) = xF(\infty)$ and two angles θ and ϕ such that $G(cos\,\theta) = y\, G(cos\,\theta = 1)$ and $T(\phi) = z\, T(\phi = 2\pi)$. In order to fix the pion kinematical variables, a random momentum $\vec{p}_N$ is chosen from the Fermi sea.

Once the kinematical variables are fixed, they are used as input in the computer simulation code for pion propagation described in refs. [14, 25] which gives us differential cross sections for every pion channel. The mentioned simulation takes into account the two possible kind of reactions in the way out of the pion: on the one hand, the pion can be absorbed, using its energy in ejecting two or more nucleons. On the other hand, the pion can "suffer" quasielastic collisions where the pion gives part of its energy to

the nucleus. In this latter case the pion can undergo charge exchange in one unit or remain with the same charge. Through double quasielastic collisions one can also have pion double charge exchange. Details can be seen in ref. [25].

3.2 Nucleons: excitation mechanisms

Nucleons can be excited in different ways through induced reactions by a virtual photon:

(i) Direct γ^*-absorption:

The virtual photon is absorbed and gives its energy to $\mathcal{N}$ nucleons. For instance, the mechanism of fig. 1(a) leads to a primary one nucleon emission, while the mechanisms of fig. 1(c) leads to a primary two nucleon emission. Details of this can be seen in ref. [23].

(ii) (γ^*, π) reactions:

Above the electropion production threshold the $\gamma^* N \to \pi N'$ reaction can occur. In this reaction (with the exception of a small fraction of coherent electropion production) one nucleon is excited. The excitation energy of the nucleon N' is small because most of the energy is used in creating the pion. Pauli blocking makes the events with more than one excited nucleon not too relevant.

(iii) (π, π') knock-out :

Once a π is produced, subsequent quasielastic collisions $N(\pi, \pi')N'$ are possible.

(iv) π absorption or indirect γ^*-absorption:

The produced π cannot only be multiply scattered but also be absorbed by $\mathcal{N}$ nucleons exchanging virtual pions or other mesons. In this case $\mathcal{N}$ must be greater than 1 and, in our approach, we consider events up to $\mathcal{N} = 3$.

(v) NN- collisions :

The number of excited nucleons increases by means of their secondary collisions. A nucleon can share its energy with another one in such a way that both remain after the interaction with energy greater than the Fermi energy. These secondary nucleons will appear mainly in the lower part of the spectrum.

Obviously, in order to explain the nucleon spectra, one must consider all these processes simultaneously.

Finally, in the next subsection we will discuss the mechanism (v) above.

We discuss here briefly how the nucleons are generated in the first two mechanisms quoted above. Those generated in the (π, π') and π absorption steps are discussed in ref. [14].

- Direct γ^*-absorption

  As we commented before, our theoretical approach allows us to determine which is the fraction of direct γ^*-absorption corresponding to one, two or three nucleons. Furthermore, it provides us with the probabilities for the different channels in each point of the nucleus. The MC selects randomly -according to the distribution of probability- which process takes place and where does it happen. In section 2 we described how the nucleon momenta and charge are generated for the $1N$ induced γ^* absorption (see fig. 1(a)). For the case of two and three nucleon induced γ^* absorption the momenta of the outgoing particles will be chosen

according to phase space distributions. Their charges will be selected according to the isospin dependence of the process. For example, the non-resonant terms (called background terms) in the absorption of the virtual photon by two nucleons, correspond mainly to absorption by pairs proton-neutron (pn) because most of them imply the exchange of a charge pion between both nucleons. Hence they have a weight proportional to $\rho_n\rho_p$ (ρ_p (ρ_n) is the nuclear density of protons (neutrons)). In some of these reactions, a π^0 is exchanged and they lead to the absorption by pairs proton-proton (pp) and neutron-neutron (nn), thus having weigths ρ_p^2 and ρ_n^2 respectively as in the case of the resonant term which has a contribution of two-body with an isospin dependence

$$\frac{1}{6}\rho_p^2 + \frac{4}{6}\rho_p\rho_n + \frac{1}{6}\rho_n^2$$

and a contribution of three-body which splits into the four possible channels according to the relatives probabilities

$$\frac{1}{18}\rho_p^3 + \frac{8}{18}\rho_p^2\rho_n + \frac{8}{18}\rho_p\rho_n^2 + \frac{1}{18}\rho_n^3$$

- Direct (γ^*, π)

  Once the virtual photon momentum is fixed, our code selects a random nucleon from the Fermi sea and chooses the charge and the momentum of the outgoing pion according to the nuclear cross section (see section 3.1). With this, all the properties of the excited nucleon are also fixed.

3.3 Nucleon propagation

The nucleons in the nucleus move under the influence of a complex optical potential. The imaginary part of the potential is related to the probability of nucleon quasielastic collisions in the nucleus (and extra pion production at higher energies which we do not consider here). We consider explicitly these collisions since they generate new nucleons going outside the nucleus. As with respect to the real part, we use it to determine the classical trajectories that the nucleons follow in the nucleus between collisions.

As done in ref. [14] we take as the real part of the nucleon-nucleus potential

$$V(r) = V_\infty - \mathcal{E}(r) = -\frac{k_F^2}{2M_N} = -\frac{1}{2M_N}\left(\frac{3}{2}\pi^2\rho(r)\right)^{2/3}$$

It represents the interaction of a single nucleon with the average potential due to the rest of the nucleons. This choice of $V(r)$ means that the total nucleon energy is the difference between its kinetic energy and the Fermi energy, ϵ_F.

As with respect to collisions in our Monte Carlo simulation we follow each excited nucleon by letting it move a short distance d such that $Pd << 1$ (P represents the probability per unit of length for a quasielastic collision). The new position ($\vec{r}\,'$) and momentum ($\vec{p}\,'$) are taken from the Hamiltonian equations as

$$\begin{cases} \vec{r}\,' = \vec{r} + \delta\vec{r} = \vec{r} + \hat{p}d \\ \vec{p}\,' = \vec{p} + \delta\vec{p}\ ;\ \delta\vec{p} = -\dfrac{\partial V}{\partial r}\dfrac{M_N d}{p}\hat{r} \end{cases}$$

which follow from the Hamilton equations or equivalently from energy and angular momentum conservation.

Our code selects randomly, according to the reaction probabilities which will be discussed in 3.4, if the nucleon is scattered or not and, in the case of scattering, what kind of process takes place. If no collision takes place, we move the nucleon again. When the nucleon leaves the nucleus we stop the process and it is counted as a contribution to the cross section. If a NN scattering is selected instead, we take a random nucleon from the Fermi sea and calculate the initial kinematical variables (P^μ and s, full four-momentum of the nucleon-nucleon system in the nuclear frame and invariant energy, respectively). Then, a $cos\,\theta_{CM}^{N'}$ is selected, according to the expression given in ref. [14]. This expression gives us the correct probability given by $d\sigma^{NN'}/d\Omega_{CM}$ (in the same appendix) plus Pauli blocking restrictions. We take also into account Fermi motion and renormalization effects in the angular dependence. We take them into account by multiplying each event by a weight factor

$$\xi = \lambda(N_1, N_2)\hat{\sigma}^{N_1N_2}\rho_{N_2}$$

where $1/\lambda(N_1, N_2)$ is the probability by unit of length that one nucleon N_1 collides with another nucleon N_2. In average, this factor ξ is equal to one.

Our method assumes that the nucleons propagate semiclasically in the nucleus. The justification of this hypothesis for real photons is given in ref. [14]. In the next section we give some detail on the evaluation of the equivalent NN cross section in the medium.

3.4 NN cross sections

We are using the parameterization of the NN elastic cross section given in the appendix of ref. [14]. Due to the fact that for particles of low momenta, the Monte Carlo induces large errors, we are not considering collisions of nucleons with kinetic energies below 50 MeV.

On the other hand, the reaction probability will change due to the nuclear medium effects (Fermi motion, Pauli blocking and medium renormalization). Then, according to ref. [14], the expression for the mean free path (λ) of the nucleon is given by

$$\frac{1}{\lambda}(N_1) = 4\int \frac{d^3p_2}{(2\pi)^3} n_{p_2}\left[\frac{Z}{A}\hat{\sigma}^{N_1p}(s) + \frac{(A-Z)}{A}\hat{\sigma}^{N_1n}(s)\right]\frac{|\vec{p}_{1\,lab}|}{|\vec{p}_1|} \tag{9}$$

with P, the full four-momentum of the NN system in the nuclear frame; $s = P^2 = (p_1 + p_2)^2$; N_1, the outgoing nucleon and N_2, the nucleon in the medium.

Furthermore,

$$\hat{\sigma}^{N_1N_2} = \int d\Omega_{CM}\frac{d\sigma^{N_1N_2}}{d\Omega_{CM}} f(q)\Theta(\kappa - |\hat{P}.\hat{p}_{CM}|) \tag{10}$$

where CM is the NN center of mass frame and

$$\kappa = x\Theta(1-|x|) + \frac{x}{|x|}\Theta(|x|-1) \tag{11}$$

On the other hand

$$x = \frac{P^0\, p^0_{CM} - \epsilon_F\sqrt{s}}{|\vec{P}\,||\vec{p}_{CM}|} \tag{12}$$

where $\vec{p}_{CM}$ is the nucleon momentum in the CM frame and ϵ_F is the Fermi energy. The function $f(q)$ corresponds to

$$f(q) = \frac{1}{\left|1 - U(q)\left(\frac{f_{\pi NN}}{m_\pi}\right)^2 V_t(q)\right|^2} \tag{13}$$

where $U(q)$ is the Lindhard function ($U(q) = U_N + U_\Delta$) and q is the momentum transfer in the nuclear frame. V_t is the spin-isospin effective interaction (details of this can be seen in ref. [23]). In these expressions, $\Theta(\kappa - |\hat{P}.\hat{p}_{CM}|)$ takes into account Pauli blocking and $f(q)$, the medium renormalization.

4 Results

4.1 $(e, e'N)$ reactions.

We show our results for the cross section of the $(e, e'p)$ process as a function of the missing energy (which is defined as $E_m = \omega - T_p$, the difference between the energy transfer and the proton kinetic energy.

In figs. 5-9 we show results for different kinematical configurations. The agreement with experiment is fair globally, although some punctual discrepancies appear for certain pieces of data. The trend of the spectrum is well reproduced, with the cross section increasing with the missing energy in the region of energies studied. The region of large missing energy comes from pion production, with or without reabsorption, and from secondary nucleons originated in the NN collisions. Some of these mechanisms, however, are more visible in the two nucleon emission as we show later.

Further results can be seen in ref.[27] which show a very good agreement between experiment and the present theory.

In fig. 10 we show a missing energy spectrum for pn emission at $\omega = 400$ MeV. We see two peaks, one at low energies and the other at energies around 250 MeV. In the figure we have also separated the different sources of contribution. The peak at low energies corresponds to the original γ^* absorption by a pair of nucleons. We include there all events corresponding to the case where the pairs leave the nucleus

without further interaction as well as those events where any of the nucleons undergoes secondary collisions. We also include the contribution from original three nucleon γ^* absorption, which in this case is relatively small.

The broad peak at high missing energies in fig.10 corresponds to original pion production. In this case one has the possibility that the pion is reabsorbed, which accounts for the largest part of the strength, while there is a fraction, wich increases with the missing energy, corresponding to the case where the pion escapes from the nucleus.

In fig. 11 we show the same figure for pp emission. The features are similar, only in this latter case the peak at low energies corresponding to primary γ^* absorption by a pair of nucleons (mostly pp) with or without FSI is about 5 to 6 times smaller than in the pn emission case. On the other hand, the broad peak at large missing energies corresponding to primary pion production is about 1/3 the size of the corresponding pn peak, much as it happened in real γ absorption.

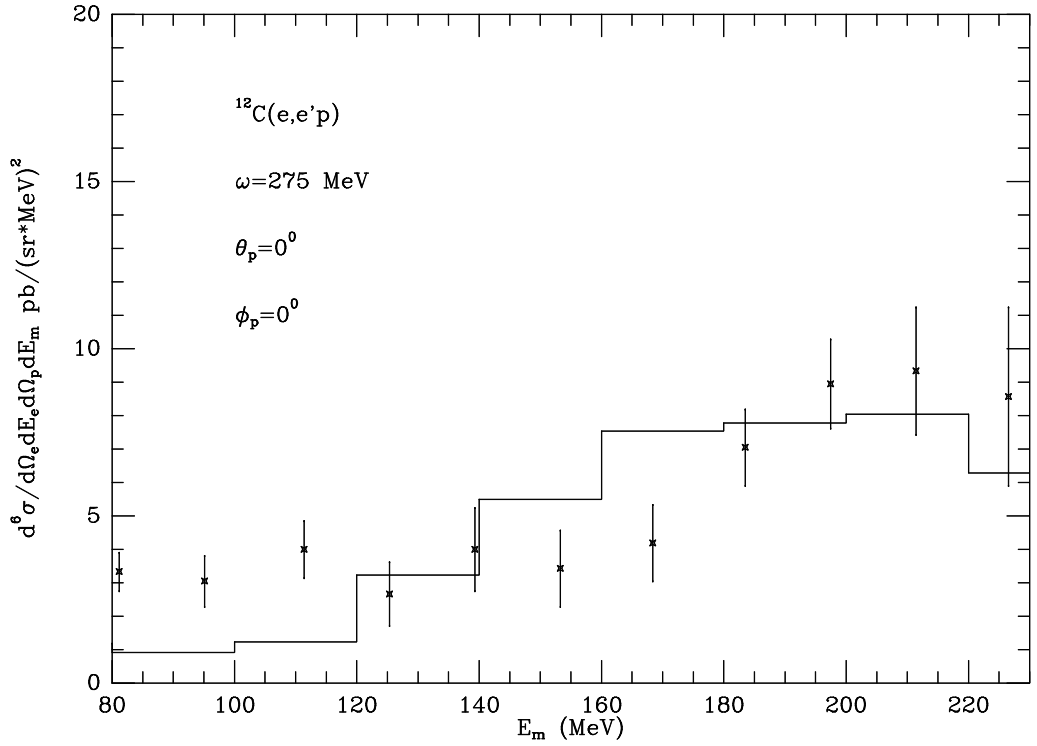

Fig.5 The $^{12}C(e,e'p)$ differential cross section as a function of the missing energy. $E_e = 460$ MeV, $\omega = 275$ MeV, $|\vec{q}| = 401$ MeV and $\theta_p = 0^0$. Experimental data from [28].

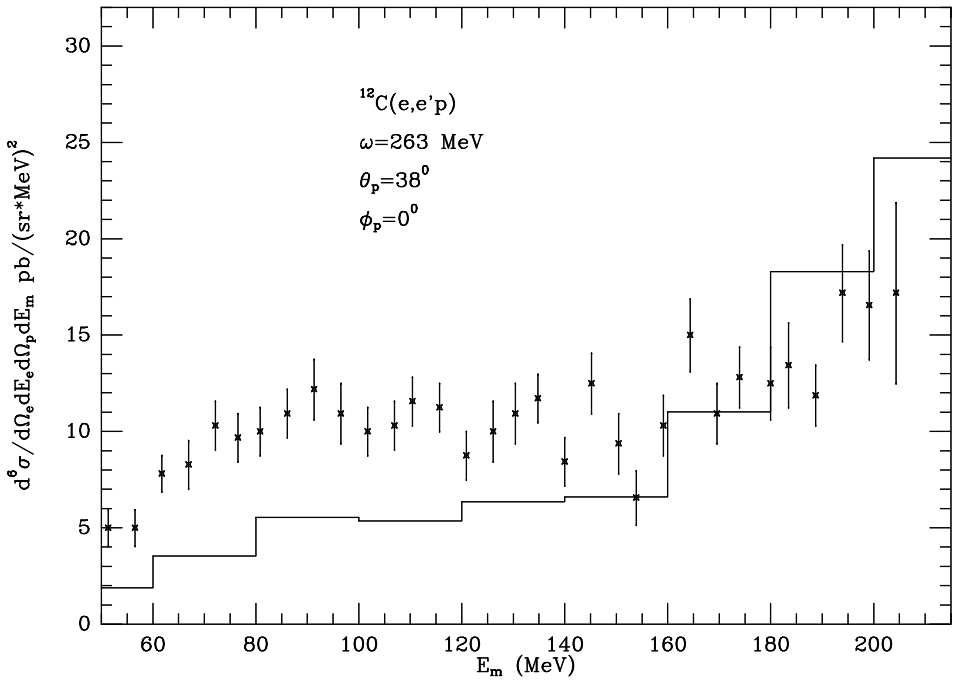

Fig.6 Same as fig.5 with $E_e = 478$ MeV, $\omega = 263$ MeV, $|\vec{q}| = 303$ MeV and $\theta_p = 38^0$. Experimental data from [10].

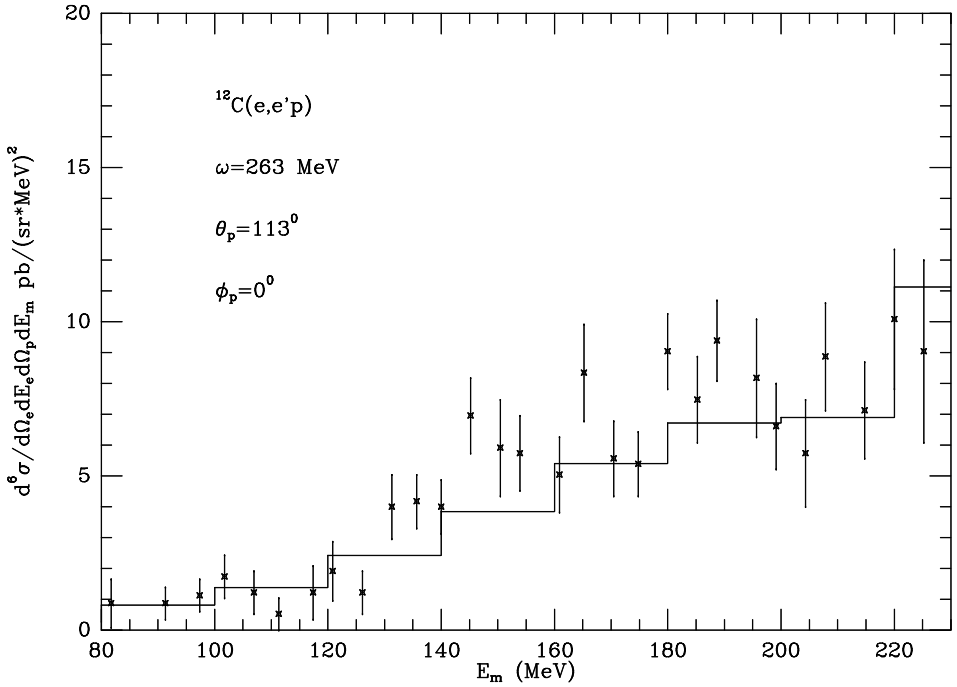

Fig.7 Same as fig.5 with $E_e = 478$ MeV, $\omega = 263$ MeV, $|\vec{q}| = 303$ MeV and $\theta_p = 113^0$. Experimental data from [10].

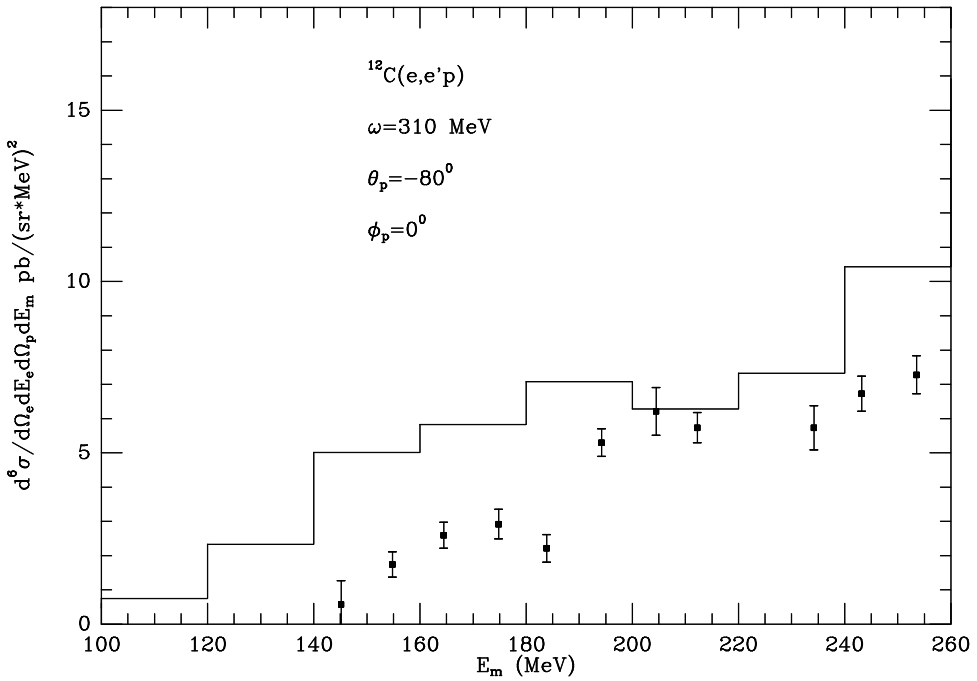

Fig.8 Same as fig.5 with $E_e = 509$ MeV, $\omega = 310$ MeV, $|\vec{q}| = 343$ MeV and $\theta_p = -80^0$. Experimental data from [29].

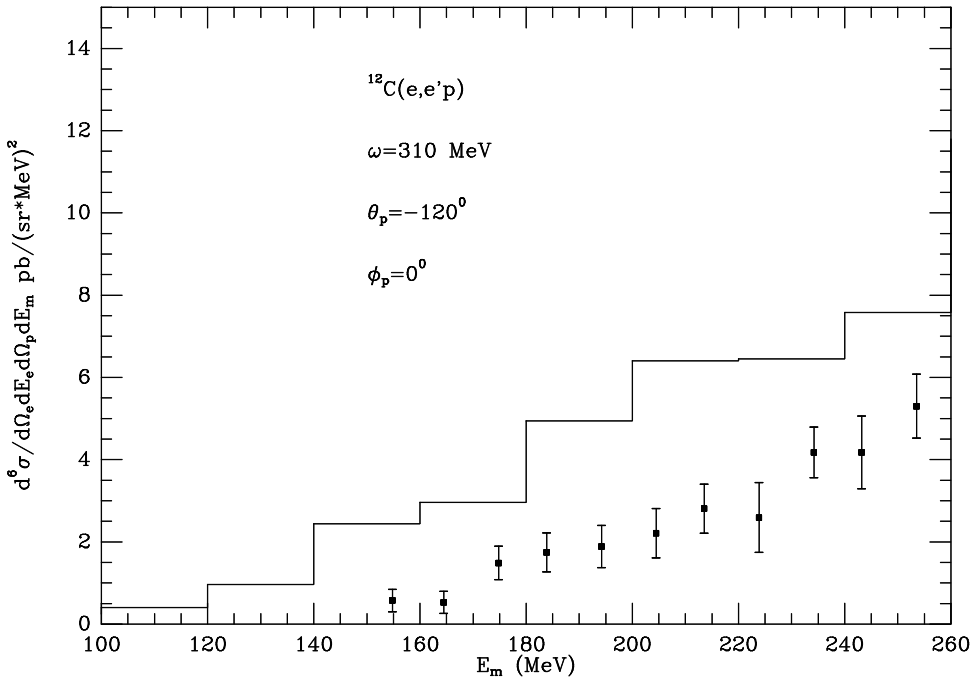

Fig.9 Same as fig.5 with $E_e = 509$ MeV, $\omega = 310$ MeV, $|\vec{q}| = 343$ MeV and $\theta_p = -120^0$. Experimental data from [29].

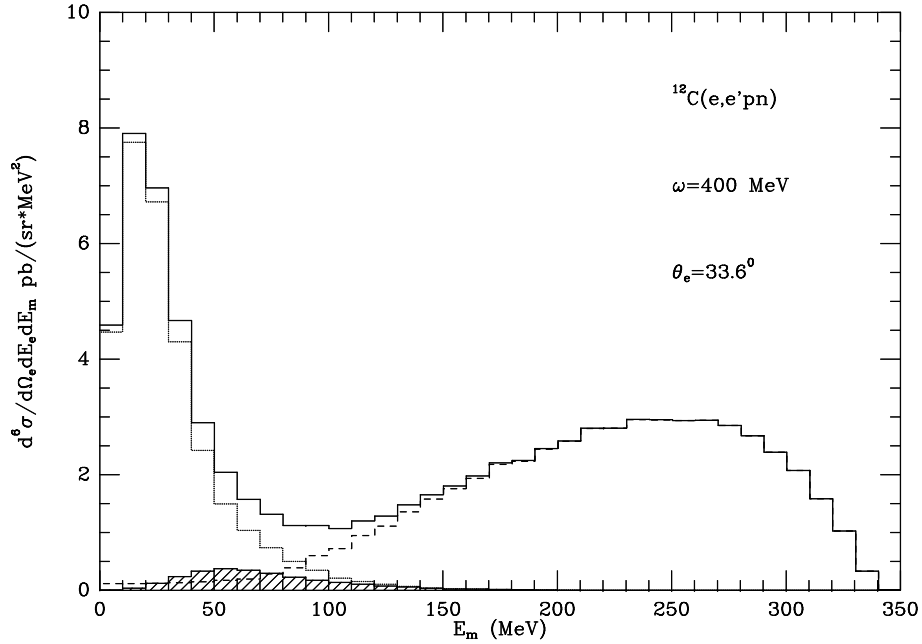

Fig.10 $^{12}C(e,e'pn)$ differential cross section as a function of the missing energy $E_m = \omega - T_{p1} - T_{p2}$. $E_e = 705$ MeV, $\omega = 400$ MeV and $\theta_e = 33.6^0$. We have separated the different contributions: 2N+FSI (main histogram at low miss. energies), 3N+FSI and 1π+FSI (main histogram at high miss. energies).

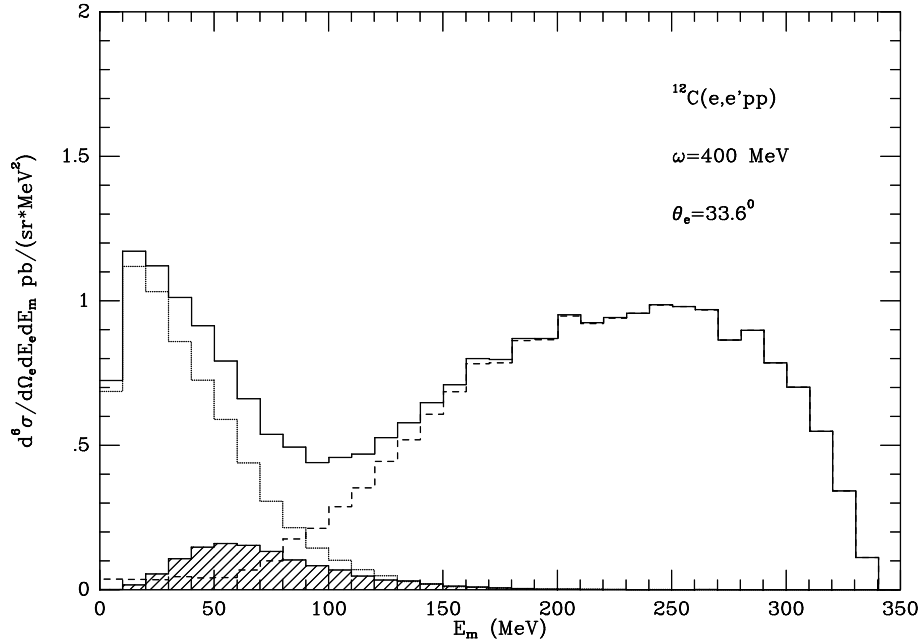

Fig.11 $^{12}C(e,e'pp)$ differential cross section as a function of the missing energy. $E_e = 705$ MeV, $\omega = 400$ MeV and $\theta_e = 33.6^0$. We have separated the different contributions: 2N+FSI (main histogram at low miss. energies), 3N+FSI and 1π+FSI (main histogram at high miss. energies).

In fig. 12 we show results for the $(e, e'\pi)$ differential cross section as a function of the pion momentum for two different angles. This corresponds to pions which manage to scape the nucleus without absorption, although they are allowed to undergo quasielastic collisions. The pion momenta peak around the resonance region where pion production has its maximun strengh.

In fig. 13 we show a picture in which we separate the primary pions produced into those which are absorbed and those which manage to escape as a function of r, the radius where they are produced. As can be seen, the pions which are produced in the interior of the nucleus are those which have more chances to be absorbed. The results are similar for other nuclei, except that the fraction of absorbed pions increases with A (see ref. [30]).

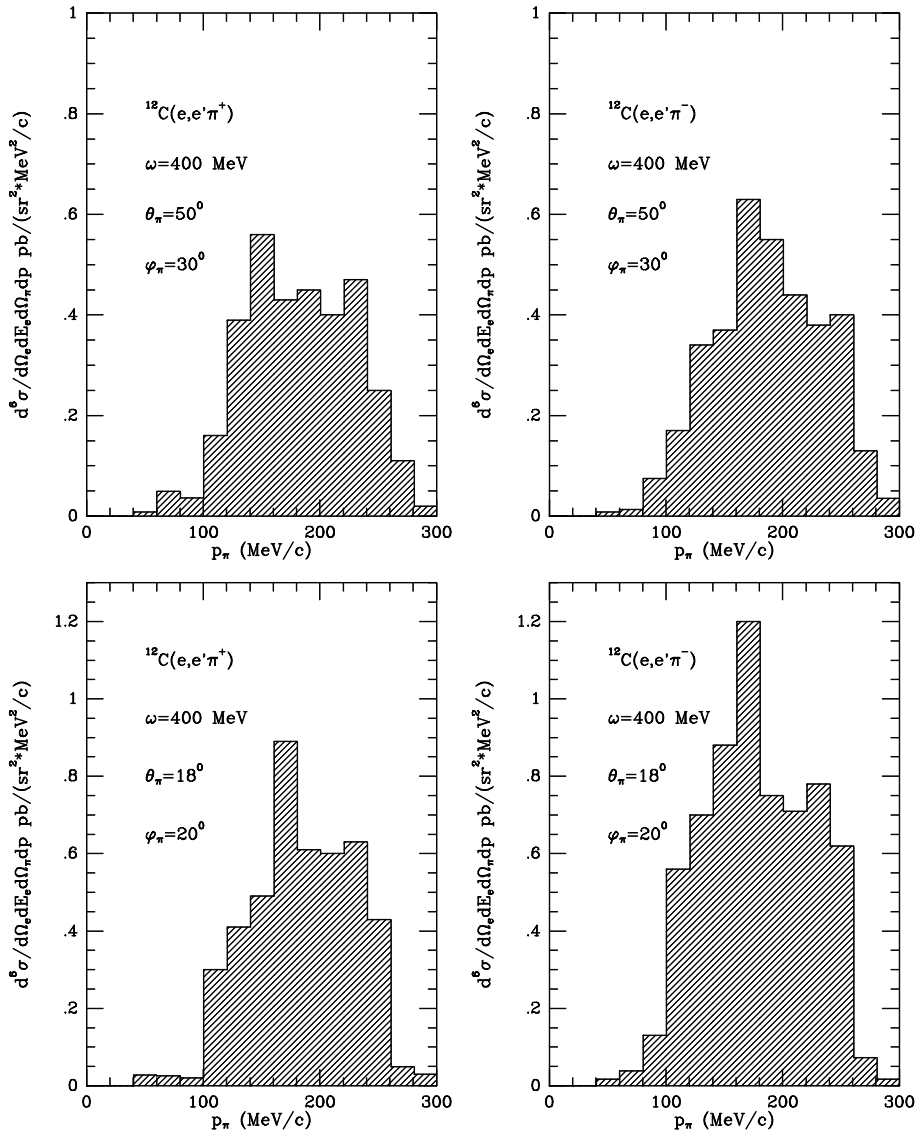

Fig.12 $^{12}C(e, e'\pi)$ differential cross section for two different angles and $E_e = 705$ MeV, $\omega = 400$ MeV and $\theta_e = 33.6^0$.

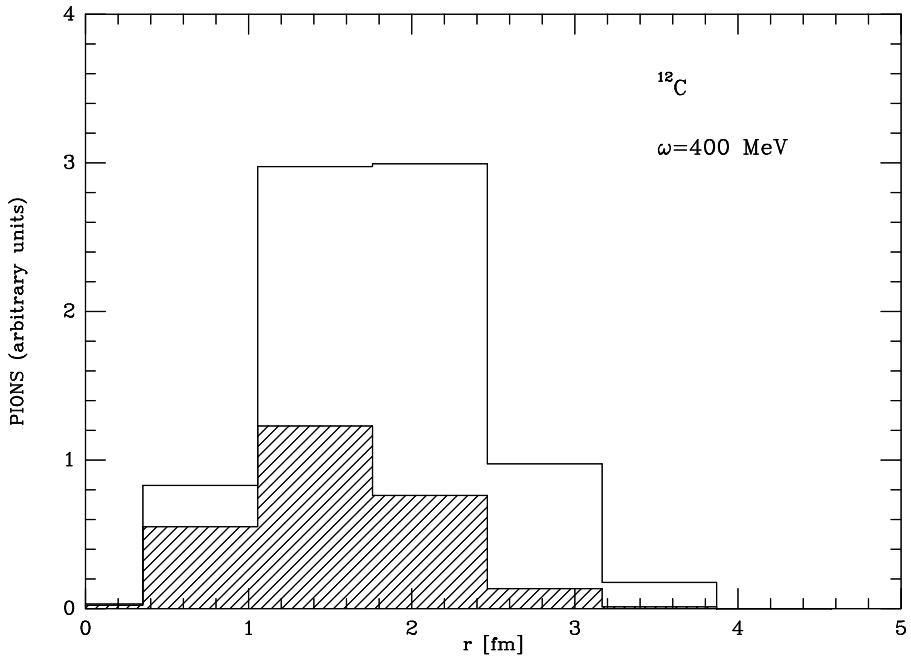

Fig.13 ^{12}C: separation of primary pions into those which are absorbed (lower histogram) and those which manage to escape (upper histogram) as a function of r. $E_e = 705$ MeV and $\theta_e = 33.6^0$.

In figs. 14,15 we show the same results but now integrated over r, as a function of ω. Figure 14 shows that in ^{12}C about one fourth of the primary pions produced are absorbed in their way out of the nucleus and the rest manages to escape. The situation is reversed in ^{208}Pb, as can be seen in fig. 15, where about two thirds of the primary pions produced are absorbed in the nucleus and onlu one third escapes.

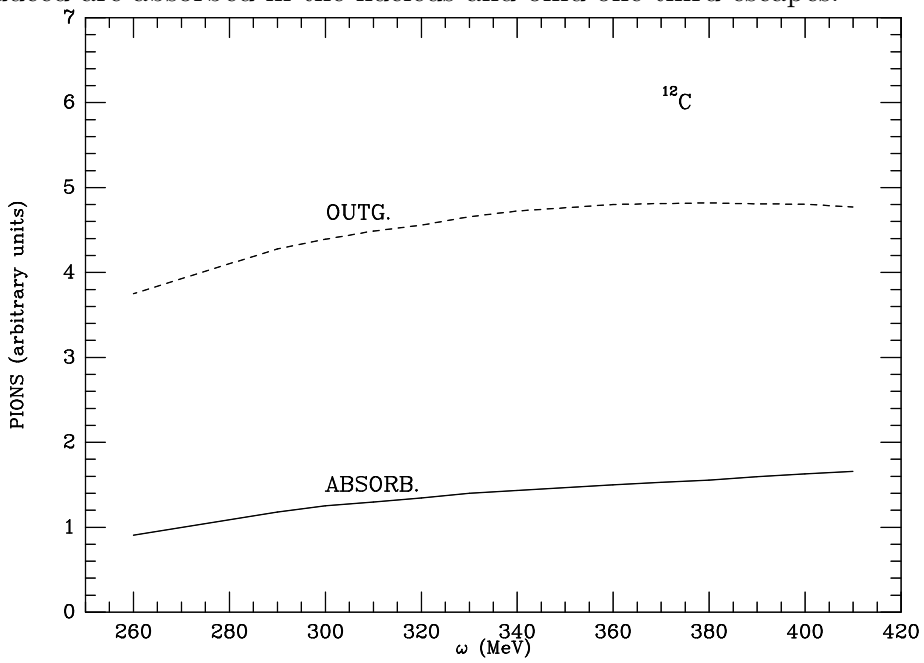

Fig.14 Same as fig. 13 integrated over r and as a function of ω. $E_e = 705$ MeV and $\theta_e = 33.6^0$.

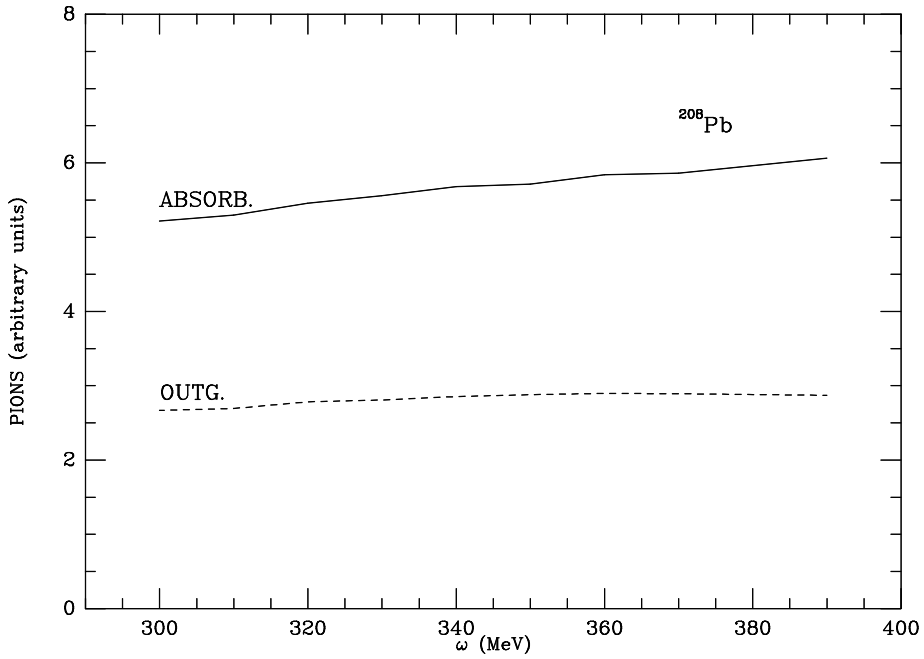

Fig.15 Same as fig. 14 for ^{208}Pb. $E_e = 705$ MeV and $\theta_e = 33.6^0$.

In fig. 16 we show the cross section for the emission of a proton and a pion in coincidence, as a function of T_p. We observe that the energies of the nucleons are relatively low, since the pion carries in this case most of the energy. At higher energies, the proton energy distribution becomes obviously more spread.

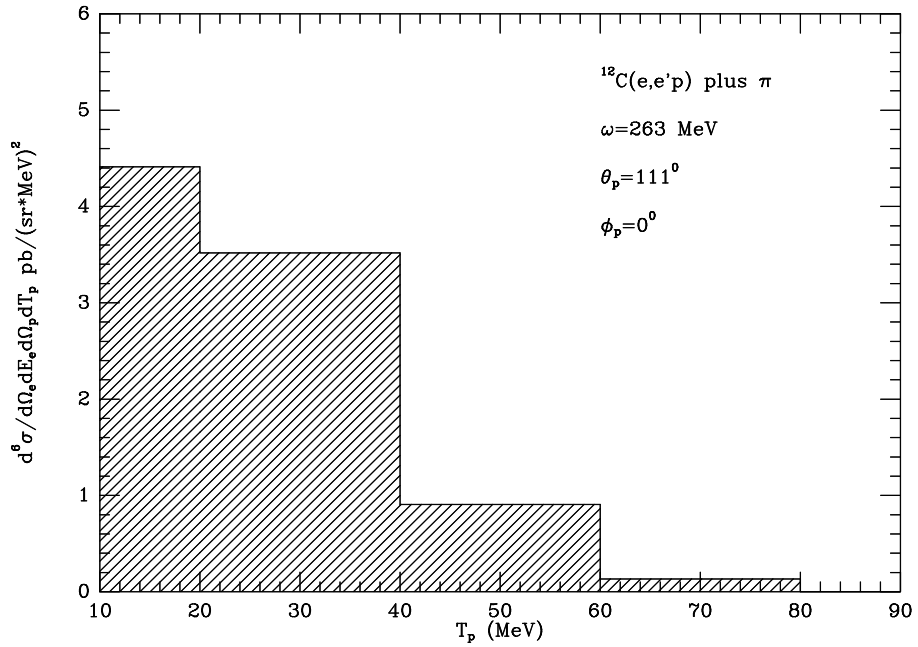

Fig.16 $^{12}C(e,e'p)$ differential cross section plus a pion detected. $E_e = 478$ MeV, $\omega = 263$ MeV, $|\vec{q}| = 303$ MeV and $\theta_p = 111^0$.

5 Conclusions

We have carried out a systematic study of different exclusive channels in the (e, e') reaction, like $(e, e'N)$, $(e, e'NN)$, $(e, e'\pi)$ and $(e, e'N\pi)$. The procedure used to deal with this multichannel problem in the final state of the (e, e') reaction, has been a Monte Carlo simulation method in which the probabilities for the different steps have been evaluated microscopically before using quantum mechanical many body techniques.

The procedure allows one to trace back to the primary step and subsequent secondary steps the different contributions to a certain final state channel. For instance, in pn emission the pn final state can come from direct knockout of a pn pair by the virtual photon. The same process with final state interaction of some of the nucleons, from three body knockout, with or without final state interaction of the nucleons. Also, from pion production in the primary step followed by pion reabsorption of the pion by pairs or trios of particles. This last process shows a strong A dependence in which the fraction of pions which are absorbed changes from 1/4 to 2/3 from ^{12}C to ^{208}Pb. This implies a pion absorption fraction proportional to A^α, with $\alpha \approx 1.3$, while in pion absorption experiments, with cross sections close to πR^2, the absorption cross section goes as A^α with $\alpha = 0.66$. This means that the indirect way of virtual photon absorption discussed above, with pion production plus reabsorption, is more sensitive to the intrinsic probability of pion absorption than the pion absorption cross section in pion nucleus collisions. In other words, one can learn more about the mechanisms of pion absorption studying indirect photon absorption (with real or virtual photons) than from pion absorption in pion nucleus experiments.

We have compared with a limited amount of experimental data here and found good agreement with experiment. Some experimental groups are comparing their data with the predictions of the present theoretical approach with good agreement so far.

The value of the present work can be seen form different points of view. From one side, the comparison with data in different kinematical regions and different channels can serve to assess the strengh of the different mechanisms discussed here. Conversely, one can use the present theoretical tool as a prospective device in order to find the kinematical situations which make it more efficient the study of certain mechanisms that one choose to investigate. A similar tool for real photons [14] has been used efficiently in both directions [18, 19, 20] and it looks clear that the present study for virtual photons can play a similar role in the future in order to extract the maximum information available form forthcoming experiments at intermediate energy labs.

Acknowledgments

We would like to acknowledge useful discussions with R. Edelhoff and G. Rosner, J. Ryckebusch and J. Segura. One of us, J. Nieves, acknowlodges to DEGS under contract PB95-1204. This work has been partially financed by CICYT contract number, AEN 96-1719.

References

[1] S. Boffi et al., Phys. Rep. 226 (1993) 1.

[2] D. G. Ireland and G. Van der Steenhoven, Phys. Rev. C 49 (1994) 2182.

[3] V. Van der Sluys et al., Phys. Rev. C 54 (1996) 1322.

[4] L.J.H.M. Kester et al., Phys. Lett. B366 (1996) 49.

[5] A. Polls et al., Phys. Rev C 55 (1997) 810.

[6] C. Giusti and F.D. Pacati, Nucl. Phys. A571 (1994) 694.

[7] J. Ryckebusch et al., Phys. Lett. B350 (1995) 1.

[8] C. Giusti and F.D. Pacati, Nucl. Phys. A535(1991) 573.

[9] C. Giusti et al., Nucl. Phys. A546 (1992) 607.

[10] J. Ryckebusch et al., Phys. Lett. B333 (1994) 310.

[11] J. Ryckebusch et al., Phys. Lett. B383 (1996) 1.

[12] S. Boffi and M.M. Giannini, Nucl. Phys. A526 (1991) 602.

[13] S. Boffi et al., Nucl. Phys. A564 (1993) 473.

[14] R.C. Carrasco et al., Nucl. Phys. A570 (1994) 701.

[15] T. Takaki, Phys. Rev. Lett. 62 (1989) 395; ibid, Phys. Rev. C39 (1989) 359.

[16] C. Giusti and F.D. Pacati, Nucl. Phys. A585 (1995) 618.

[17] R.C. Carrasco et al., Nucl. Phys. A536 (1992) 445.

[18] G.E. Gross et al., Nucl. Phys. A593 (1995) 463.

[19] P.D. Harty et al., Phys. Lett. B380 (1996) 247.

[20] T. Helh, Prog. Part. Nucl. Phys. 34 (1995) 385.

[21] J. Arends et al., Nucl. Phys. A454 (1986) 579; H. Rost PhD thesis, University of Bonn, 1980.

[22] R.C. Carrasco et al., Nucl. Phys. A541 (1992) 585.

[23] A. Gil, J. Nieves and E. Oset, submitted to Nucl. Phys. A.

[24] J. Jourdan, Phys. Lett. B353 (1995) 189; ibid, Nucl. Phys. A603 (1996) 117.

[25] L.L. Salcedo et al., Nucl. Phys. A484 (1988) 557.

[26] C. Itzykson and J.B. Zuber, *Quantum Field Theory*, Mc Graw-Hill,1980.

[27] R. Edelhoff, Proc. of 3^{rd} Int. Workshop on Electromagnetically Induced 2N Emission, Glasgow, June 1997.

[28] H. Baghaei et al., Phys. Rev. C39 (1989) 177.

[29] A. Zondervan et al., Nucl. Phys. A587 (1995) 697.

[30] A. Gil, PhD thesis, University of Valencia, 1996.